Biochimica et Biophysica Acta 1838 (2014) 445–455

Contents lists available at ScienceDirect

Biochimica et Biophysica Acta

journal homepage: www.elsevier.com/locate/bbamem

Carboxyl-terminated PAMAM dendrimer interaction with 1-palmitoyl-2-oleoyl phosphocholine bilayers ☆

Kervin O. Evans *, Joseph A. Laszlo, David L. Compton

Renewable Product Technology Research Unit, National Center for Agricultural Utilization Research, Agricultural Research Service, U.S. Department of Agriculture, 1815 N. University Street, Peoria, IL 61604, USA

ARTICLE INFO

Article history:
Received 11 February 2013
Received in revised form 14 August 2013
Accepted 16 August 2013
Available online 28 August 2013

Keywords:
1-Palmitoyl-2-oleoyl phosphocholine bilayer
Carboxyl-terminated dendrimer
QCMD
Fluorescence
AFM

ABSTRACT

Polyanionic polymers and liposomes have a great potential use as individual drug delivery systems and greater potential as a combined drug delivery system. Thus, it is important to better understand the interactions of polymers with phospholipid bilayers. A mechanistic study of the interaction between carboxyl-terminated poly(amidoamine) (PAMAM) dendrimers with 1-palmitoyl-2-oleoyl-phosphatidylcholine (POPC) bilayer using fluorescence leakage and quartz crystal microbalance with dissipation monitoring (QCMD) was conducted. Fluorescence leakage experiments demonstrated that carboxyl-terminated generation 2 (G_2-COOH) dendrimers caused increased liposome leakage with increasing dendrimer concentration over a 0 to 20 μM range. Generation 5 (G_5-COOH), on the other hand, reduced leakage over the same concentration range, presumably by increasing lipid packing. QCMD and atomic force microscopy (AFM) measurements demonstrated that G_2-COOH interacting with supported bilayers resulted in small defects with some mass loss and no adsorption. In contrast, G_5-COOH interaction with a bilayer resulted in adsorption and local bilayer swelling.

Published by Elsevier B.V.

1. Introduction

Recent years have seen a flurry of research into using liposomes [1–4] and dendrimers as separate drug delivery systems [5–8]. Liposomes are thin shells (bilayers) of lipids that are capable of encapsulating hydrophilic and hydrophobic active agents either within their internal medium or within their bilayer, respectively, and have a demonstrated effectiveness of delivering drugs for percutaneous adsorption [9]. However, hydrophilic agents encapsulated within liposomal aqueous media can potentially interact with the headgroups of the bilayer, and hydrophobic agents partitioned within the bilayer can change the physical characteristics (e.g. fluidity and permeability) of the liposome. Thus, liposomal systems present challenges that make them less than ideal as active ingredient delivery systems.

Alternatively, dendrimers do not have the liposomal issues of fluidity and permeability. Dendrimers are polymers containing a central core shell with repeating units [8] that branch outward from the core and allow the polymer to vary in size. The branching creates microcavities between the repeating units in which active agents can encapsulate. In addition, the branching units terminate with a variety of functional groups, which allow covalent bonding of active agents. The ability to encapsulate and bind active agents makes dendrimers promising delivery systems; however, active agents can be vulnerable to degradation and early release. Thus, combining liposomes and dendrimers into a single, binary delivery system could potentially overcome the deficiencies present in each of the individual systems [10].

The past one and a half decades have seen flurry of research aimed at understanding the interaction between liposomes and dendrimers, the bulk of which focused on membrane–dendrimer interactions to better understand the efficacy of dendrimers with cells. For instance, interaction studies of single-phospholipid liposomes with cationic (amine-terminated) dendrimers were conducted by several groups like Ottaviani et al. (1998, 1999) [11–13]; Zhang and Smith (2000) [12]; Hong et al. (2004) [14]; Mecke et al. (2005) [15,16], consistently demonstrating the disruptive nature of amine-terminated dendrimers ranging in size from generation 3 (G3) to generation 7 (G7). It was also demonstrated that the disruptive nature of amine-terminated dendrimers was affected by the phase state [15,17] and charge of the membrane [12]; not to mention, it was demonstrated that dendrimers could alter the phase state of liposomes [18–20]. Further studies demonstrated that the defects created in phospholipid bilayers were the result of the formation of dendrimers–lipid aggregates or "dendrosomes" [21,22].

Discovery of the dendrimers–lipid interactions led many to explore the possibility of using the dendrimers–lipid complexes as drug delivery systems. One of the earliest studies exploring dendrimers–lipid complexes as drug-delivery systems involved amine-terminated

☆ Mention of trade names or commercial products in this publication is solely for the purpose of providing specific information and does not imply recommendation or endorsement by the U.S. Department of Agriculture. USDA is an equal opportunity provider and employer.

* Corresponding author. Tel.: +1 309 681 6436; fax: +1 309 681 6040.
E-mail address: Kervin.Evans@ars.usda.gov (K.O. Evans).

0005-2736/$ – see front matter. Published by Elsevier B.V.
http://dx.doi.org/10.1016/j.bbamem.2013.08.012

dendrimers complexed with a drug (methotrexate) and encapsulated within liposomes [23]. Khopabe et al. (2002) demonstrated that generation 4 (G4) dendrimers encapsulated within liposomes gave the highest drug entrapment. Follow-up work conducted by Papagiannaros et al. (2005) [24] demonstrated that a different G4 dendrimer–drug complex could be attached to instead of encapsulated by liposomes to increase drug incorporation efficiency and bioactivity against cancer cells. Another unique approach used G4 dendrimers to complex with lipid films to make layer-by-layer films for possible drug delivery [25]. The most recent unique use of dendrimers–liposome complexes as potential drug delivery systems involved what is termed as "liposomal locked-in dendrimers" or LLDs, which are liposomes created in the presence of dendrimers. The authors used carboxyl-terminated G4 dendrimers to form LLDs [26] and demonstrated their physico-chemical factors.

A review of the literature showed that although there is a myriad of work entailing the use of amine-terminated dendrimers with phospholipid bilayers [12,15,16,22,27–30], only a small, limited amount of work highlighting the interactions between phospholipid bilayers/carboxyl-terminated dendrimers (G_n-COOH where n is the generation number) was done. For instance, it was demonstrated that G_7-COOH disrupted DMPC bilayers in water with 100 mM NaCl [31]. Shcharbin et al. (2006) demonstrated that $G_{4.5}$-COO^- (deprotonated carboxyl-terminated dendrimers G_n-COOH) did not disturb gel phase egg yolk phosphocholine in potassium buffer solution at pH 7.4 [32]. Kelly et al. (2008) modeled G_3-COO^- with DMPC to show that G_3-COO^- extends its hydrophobic core as it approaches a fluid bilayer [33] and flattened out [17], whereas it remained spherical when adsorbed onto gel-phase membrane [17]. Based on this small pool of work, there is not enough information to make any conclusions about the general interactions between G_n-COOH and phospholipid membranes. For example, does the size of G_n-COOH dictate the interaction with a membrane like it does for G_n-NH_2 [16,22]?

Our goal in this work was to understand interactions between carboxyl-terminated dendrimers and a phospholipid membrane, 1-pamitoyl-2-oleoyl-phosphatidylcholine (POPC), to better predict the behavior of potential dendrimer–liposome delivery systems. This work focused on anionic (carboxyl-terminated) PAMAM which was found to have a lower cell toxicity than cationic (amino-terminated) PAMAM [8,29]. Particularly, concentrations of dendrimers chosen for this work were well below levels found toxic for cells [29]. POPC was chosen because it has equal molar amounts of saturated/unsaturated acyl changes per mole of phospholipid which allows the bilayer to remain in the fluid phase at 37 °C. Fluorescence spectroscopy, quartz crystal microbalance with dissipation monitoring (QCMD), and atomic force microscopy (AFM) were used to describe the interaction of generation 2 (G_2-COOH) and generation 5 (G_5-COOH) dendrimers with free liposomes and supported bilayers composed of 1-palmitoyl-2-oleoyl-phosphocholine (POPC).

2. Experimental details

2.1. Reagents and materials

Poly(amidoamine) (PAMAM) carboxylated second generation (G_2-COOH; MW ~ 2935) and fifth generation (G_5-COOH; MW ~ 26,252) dendrimers, cobalt (II) chloride hexahydrate, ethylenediaminetetraacetic acid disodium dihydrate (EDTA), and octaethylene glycol monododecyl ether ($C_{12}E_8$) were purchased from Sigma-Aldrich. 1-Palmitoyl-2-dioleoyl-*sn*-glycero-3-phosphocholine (POPC) was bought from Avanti Polar Lipids (Alabaster, AL). High purity calcein was obtained from Invitrogen (Carlsbad, CA). HEPES, Sephadex G-75 column beads, columns and sodium chloride were obtained from Fisher Scientific.

2.2. Lipid preparation and formation of unilamellar phospholipid liposomes

Lipid mixtures and liposomes were prepared as described previously [34] with modification. Lipids were prepared from appropriate amounts of POPC in chloroform. POPC solutions were dried under a stream of argon and then placed under vacuum overnight. The dried lipids were rehydrated in the appropriate buffer and mixed periodically to form multilamellar phospholipid liposomes. The liposomes were subjected to five freeze–thaw cycles and 11 extrusion cycles through two 30-nm filters to form unilamellar liposomes. Liposomes were covered with argon, protected from light and stored at 4 °C until use.

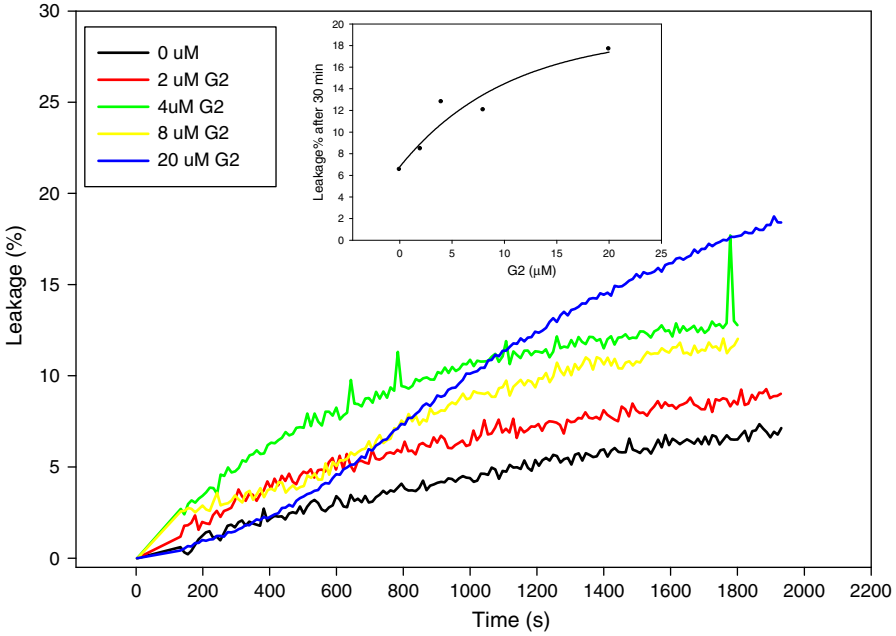

Fig. 1. Time-course dependence of calcein–cobalt leakage from POPC liposomes in the presence of increasing concentrations of G2 PAMAM dendrimers. Inset displays the leakage percent after 30 min for each G2 concentration. Data represent the mean values of 2–4 experiments.

Table 1
Leakage rate constants of POPC liposomes in the presence of increased concentrations of G2 or G5 PAMAM dendrimers (values are the average of 3 or 4 independent measurements ± S.D.). Items marked with asterisks are considered to be statistically different ($P < 0.05$) from the control (no dendrimer present) sample.

	PAMAM dendrimer (μM)	Leakage rate constant[a] ($\% s^{-1} 10^{-3}$)
G2	0	0.49 ± 0.39
	2	0.63 ± 0.31
	4	1.47 ± 0.44*
	8	4.58 ± 1.61*
	20	3.13 ± 0.76*
G5	2	0.96 ± 0.03
	4	0.40 ± 0.25
	8	0.37 ± 0.04
	20	0.66 ± 0.16

[a] Leakage rate constant reported as the mean and standard deviation of 2–4 experiments. Items marked with an asterisk are considered to be statistically different ($P < 0.05$) from the control (no PAMAM) sample.

2.3. Dynamic light scattering (DLS)

Liposome size was determined using a Nicomp submicron particle sizer (Particle Sizing Systems, Inc.; Santa Barbara, CA). Liposomes were diluted to 0.1 mM phospholipid in buffer and allowed to equilibrate to ambient temperature. Volume-weighting mode was used to calculate liposome size. Sizing was done in triplicate. Liposomes extruded at 30-nm were found to have a diameter of 46 ± 9 nm.

2.4. Liposome leakage (calcein–cobalt)

Liposomes were evaluated for membrane integrity using a leakage assay described previously [34,35]. Briefly, the leakage assay used entrapped calcein–cobalt complex that has a low fluorescent signal. As calcein–cobalt leaks from the liposomes, external EDTA binds cobalt and free calcein fluorescence increases. Buffer solutions were modified as follows: the encapsulated leakage buffer contained 1 mM calcein, 2.4 mM $CoCl_2$, 10 mM HEPES, pH 7.4; the column (external) buffer contained 10 mM HEPES, 10 mM EDTA, pH 7.4. Fluorescence was monitored using a Fluorolog 3–21 (Horiba-Jobin Yvon) fluorometer where samples were continuously stirred in 1-cm path length quartz cuvettes at 37 °C (measurements taken for 30 min at 5-s intervals). Measurements were repeated in quadruplicates. Leakage percentage (L) was defined as

$$L = \frac{F_t - F_0}{F_{max} - F_0} * 100, \quad (1)$$

where F_t was the fluorescent signal over time, F_0 was the extrapolated initial signal at time zero, and F_{max} was the fluorescent signal at the end of the experiment after rupture by addition of $C_{12}E_8$ solution. The equation $L_t = L_\infty\ (1 - \exp(-kt))$ was used to fit the data and obtain apparent rate constant k (ms^{-1}) and maximum extent of liposome leakage (L_∞) prior to liposome rupture where appropriate.

2.5. Atomic force microscopy (AFM)

AFM imaging was obtained in HEPES buffer (10 mM HEPES, 100 mM NaCl, pH 7.4) using a Nanoscope IV controller (Bruker, Santa Barbara, CA). Images were scanned at a rate of 1 Hz. Liposomes were exposed to cleaned silica wafers (Wafer World, Inc., West Palm Beach, FL) and allowed to form a supported phospholipid bilayer (SPB). Excess liposomes were gently rinsed away. Dendrimers at appropriate concentrations were slowly and gently flowed into the cell via a 1-mL syringe and images were scanned 15 min later.

2.6. Quartz crystal microbalance with dissipation (QCMD) monitoring

Monitoring of liposome adsorption onto silica surfaces was accomplished using a QCM-E4 electronic system (Q-Sense, Inc., Västra Frölunda, Sweden) [36]. A negative shift in the resonance frequency of the crystal occurred when material adsorbed to the crystal surface. Thus, frequency shift (Δf) correlated to mass adsorbed onto the sensor crystal. The adsorbed layer of mass not only caused a shift in the resonance frequency, but also caused the resonance frequency overtones to dampen and lose energy through frictional losses [37]. This loss in energy, or dissipation (ΔD), was large (typically $>1 \times 10^{-6}$) when the adsorbed mass was "soft," and ΔD was low ($<1 \times 10^{-6}$) when the adsorbed mass was stiffly bound.

Preheated (37 °C) buffer (10 mM HEPES, 100 mM NaCl, pH 7.4) was passed over the crystals prior to measurements to equilibrate the system. Once the signal remained stable for about 10 min (Δf < 1 Hz), preheated liposome samples were passed over the crystals. Liposomes formed a supported bilayer (SPB) within minutes of adsorption. Data consisted of the acquisition of the fundamental frequency (5 MHz) and the 3rd, 5th, 7th, 9th, 11th, and 13th overtones (15, 25, 35, 45, 55, 65 MHz). All measurements were conducted at 37.0 ± 0.3 °C.

The response of the resonance frequency of the quartz crystal microbalance depended on the total oscillating mass adsorbed to the sensor surface. Adsorption of solutes from the contacting buffer medium resulted in a decrease in frequency. If the attached mass was thin

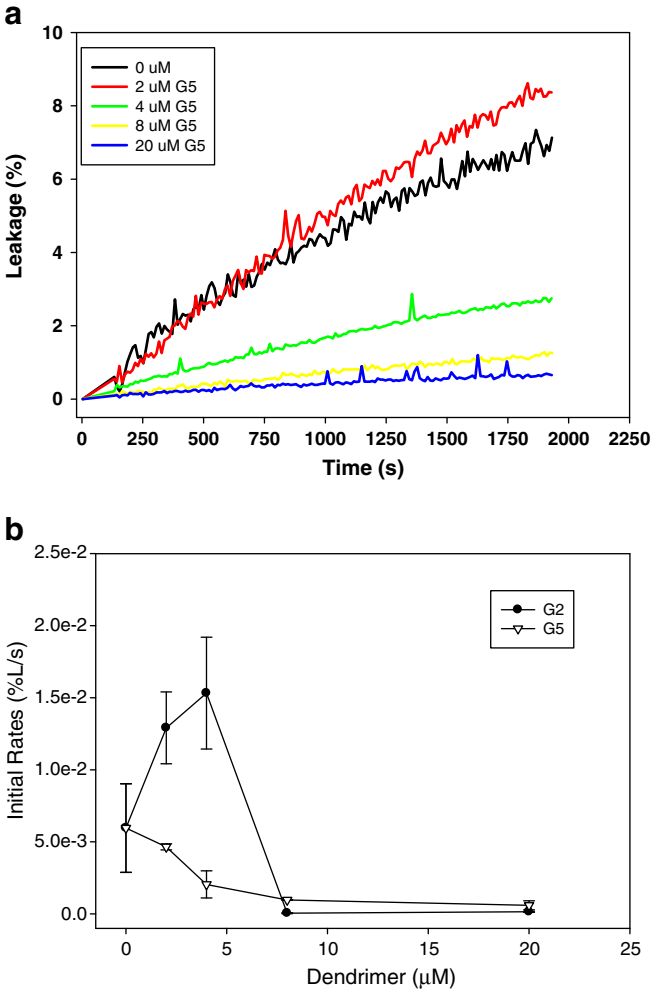

Fig. 2. (a) Time-course dependence of calcein–cobalt leakage from POPC liposomes in the presence of increasing concentrations of G5 PAMAM dendrimers. Data represent the mean values of 2–4 experiments. (b) Comparison of initial rates from G_2-COOH and G_5-COOH leakage experiments.

(≪300 μm) in comparison to the crystal and rigid, then the mass could be calculated by the Sauerbrey equation [37]. The Sauerbrey equation is

$$\Delta m = \frac{-C \times \Delta f}{n}, \quad (2)$$

where C = 17.7 ng/cm^2/Hz for a 5 MHz sensor crystal and n is the overtone number (1 for 5 MHz, 3, 5, 7, 9, 11, and 13 for the 3rd, 5th, 7th, 9th, 11th, and 13th overtones respectively). This calculation of adsorbed mass has been proven to be valid for thin lipid bilayers ($\Delta D < 1 \times 10^{-6}$) and just slightly under representative (~5%) for adsorbed unruptured liposomes ranging in thickness of several nanometers ($\Delta D \geq 1 \times 10^{-6}$) [38,39].

3. Results and discussion

3.1. Liposome leakage

Calcein–cobalt release from liposomes has been established as a useful method for determining phospholipid membrane permeability in the presence of aqueous molecules [35] and incorporated lipids [40]. Various concentrations of G_2-COOH and G_5-COOH PAMAM dendrimers were mixed with POPC liposomes containing the calcein–cobalt complex and fluorescence was used to monitor POPC liposome stability. Fig. 1 demonstrates the percentage of leaked contents caused by the presence of G_2-COOH dendrimers interacting with POPC liposomes. With no G_2-COOH present, POPC liposomes had an extent of leakage that was approximately 6.8%. The addition of 2 μM G_2-COOH resulted in leakage that was just slightly faster (though statistically similar; Table 1) than leakage without G_2-COOH present. The addition of G_2-COOH also resulted in a slightly greater extent of leakage (~8.9%). Liposome leakage rate and extent of leakage increased upon the addition of 4 μM G_2-COOH, indicating that G_2-COOH at 2 and 4 μM increasingly disturb POPC bilayers (Table 1). The leakage data, however, developed a shape other than an "exponential-rise-to-maximum" after 8 μM G_2-COOH was mixed with leakage liposome. No longer could a single-exponential rise-to-maximum fit the data as was done for 2 and 4 μM data, and a double-exponential did not well describe the data either. Data resulting from liposomes interacting with 20 μM G_2-COOH displayed a similar but more pronounced shape as that for 8 μM G_2-COOH. This shape in the leakage data has been described as a "stretched exponential" and considered to be due to aggregation [41,42]. Fitting the data to "stretched exponential" for kinetic analysis proved complex. Therefore, the data for 8 and 20 μM G_2-COOH were instead fit to a sigmoidal curve. Consequently, the discussion of kinetics analysis will focus on initial rates of the leakage process from henceforth. As for the extent of leakage, it continued to show a dependence on G_2-COOH concentration (Fig. 1, inset). The

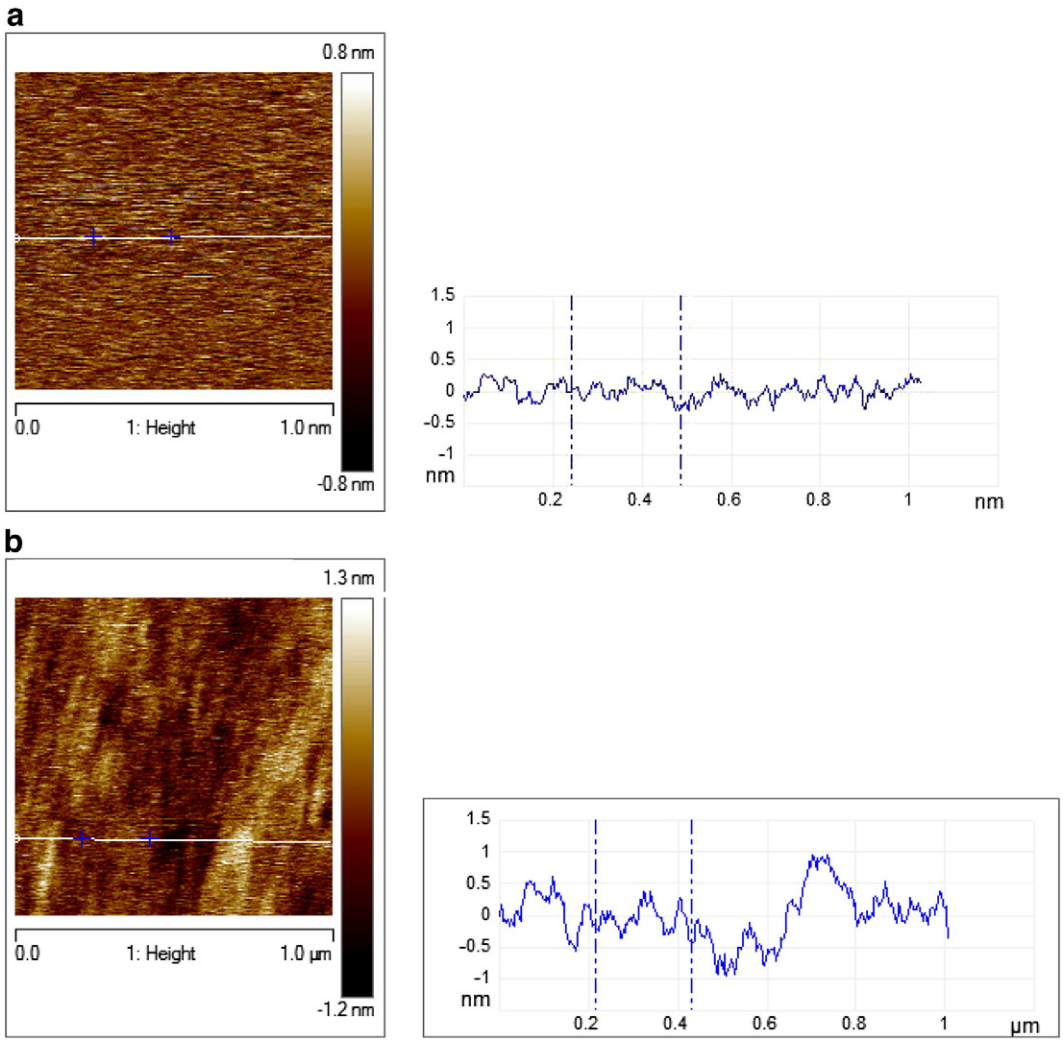

Fig. 3. AFM images of POPC bilayer after exposure to (a) 0, (b) 2, (c) 4, (d) 8, and (e) 20 μM G_2-COOH PAMAM dendrimers in 10 mM HEPES, pH 7.4. Images were acquired at 1 Hz scan rate and corresponding section analysis is shown.

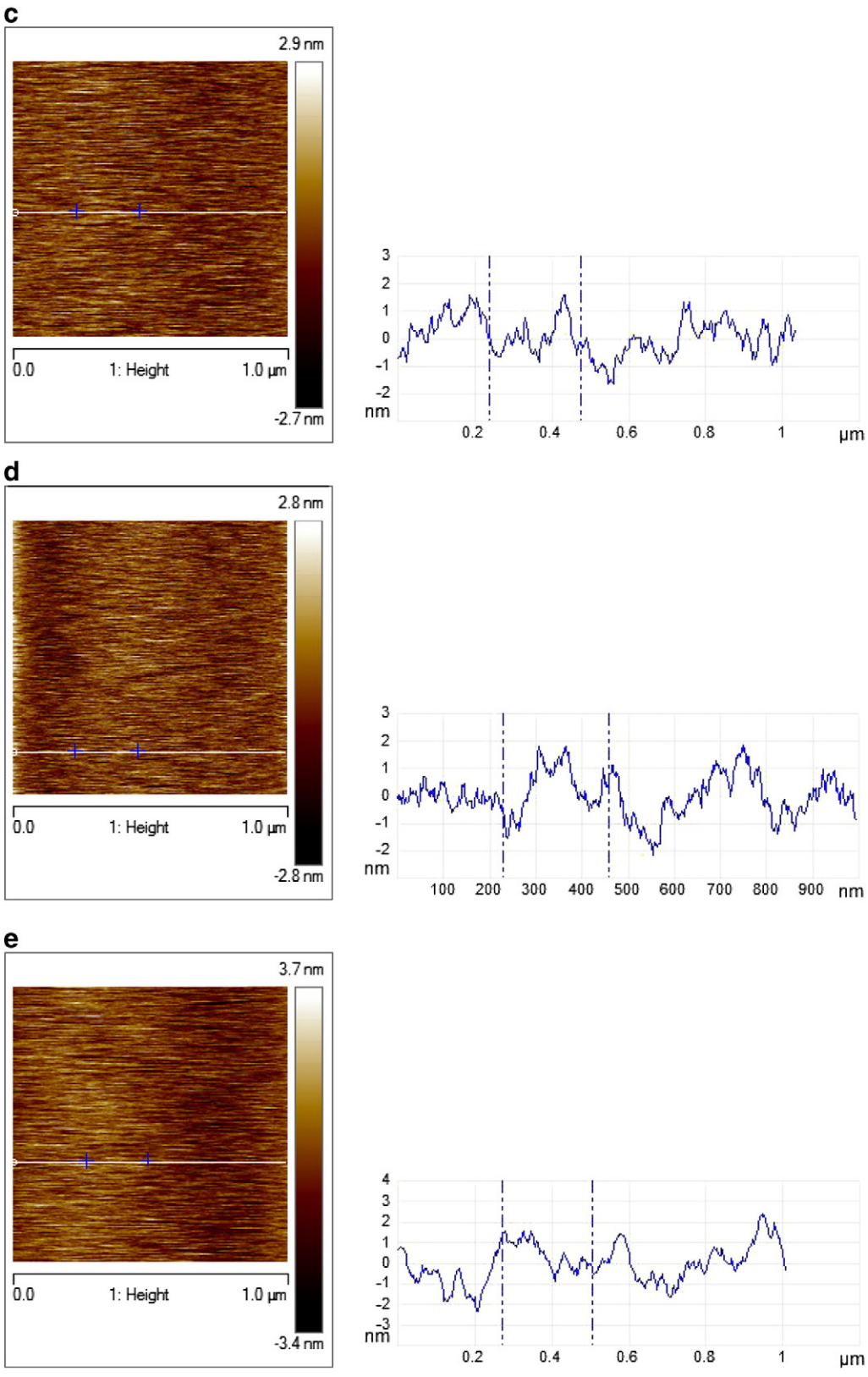

Fig. 3 (*continued*).

concentration dependence of the extent of leakage demonstrates that G_2-COOH interacts with bilayer [43], possibly through electrostatic interactions [12,14,17].

Contrastingly, POPC liposomes exposed to G_5-COOH PAMAM dendrimers at the same concentrations (2, 4, 8 and 20 μM) demonstrated reduced leakage. Fig. 2a demonstrated the leakage percentage of POPC liposomes in the presence of increasing concentration of G_5-COOH PAMAM dendrimers. At all G_5-COOH concentrations explored, POPC liposomes experienced statistically the same leakage rate and a correlated decreased leakage percentage. The simplest explanation for this

decreased leakage percentage is that lipid packing was increased in the presence of G_5-COOH dendrimers as it has been demonstrated that increased lipid packing reduces aqueous content leakage [44].

The strikingly different behaviors of G_2-COOH and G_5-COOH were further illustrated in the kinetics analysis using the initial rates of leakage (Fig. 2b). Initial rate plotted versus dendrimer concentration showed an increase with G_2-COOH concentration up to 4 μM, above which there was a sudden decrease in the initial rate. This suggests that leakage was retarded by the presence of high concentrations (8 and 20 μM) of G_2-COOH, possibly inducing aggregation. There are two possibilities for aggregation: the first possibility is that liposomes started to aggregate in the presence of a high concentration of negatively charged G_2-COOH (8 and 20 μM); or the second one is that the high concentration of negatively charged G_2-COOH aggregated in the presence of the Co^{2+}. Liposomal aggregation was ruled out by dynamic light scattering (DLS) measurements that showed liposomes incubated (for at least 10 min) with either 8 or 20 μM G_2-COOH in the absence or presence of Co^{2+} did not vary in size from liposomes without G_2-COOH (data not shown). This made the latter possibility more likely, although G_2-COOH aggregation could not be ruled out or confirmed because DLS intensity was too low (DLS signal for G_2-COOH was higher than buffer background but well below the minimum value for accurate sizing, indicating aggregates were too small and/or too few). G5-COOH, on the other hand, displayed decreasing initial rates with decreased dendrimer concentration, consistent with increased lipid packing that would limit the efflux of solutes from the interior of liposomes.

3.2. AFM imaging

The interaction between G_2-COOH or G_5-COOH dendrimer and a SPB was further explored using AFM imaging. Fig. 3 displays the results of the interaction between a POPC SPB and G_2-COOH dendrimers. Fig. 3a shows the SPB prior to G_2-COOH exposure where no defects or undulations were found (roughness was 0.23 ± 0.02 nm). Fig. 3b–e shows the SPB in the presence of 2, 4, 8, and 20 μM G_2-COOH, respectively. The SPB in the presence of 2 μM G_2-COOH displayed small defects (dark areas) and an undulation pattern (Fig. 3b; roughness 0.33 ± 0.03 nm). The cross-section analysis (adjacent to Fig. 3b) revealed that the defects and undulations were not more than 1 nm below or above the planar surface of the SPB, respectively. POPC SPB exposed to 4, 8 or 20 μM (Fig. 3c, d, e, respectively) revealed smaller defects and an increase in surface roughness (0.77 ± 0.07 nm, 0.83 ± 0.04 nm and 0.93 ± 0.14 nm, respectively). Undulations and defects approached 2 nm high or 2 nm deep, respectively, indicating that part of the top monolayer of lipids was disturbed and possibly removed.

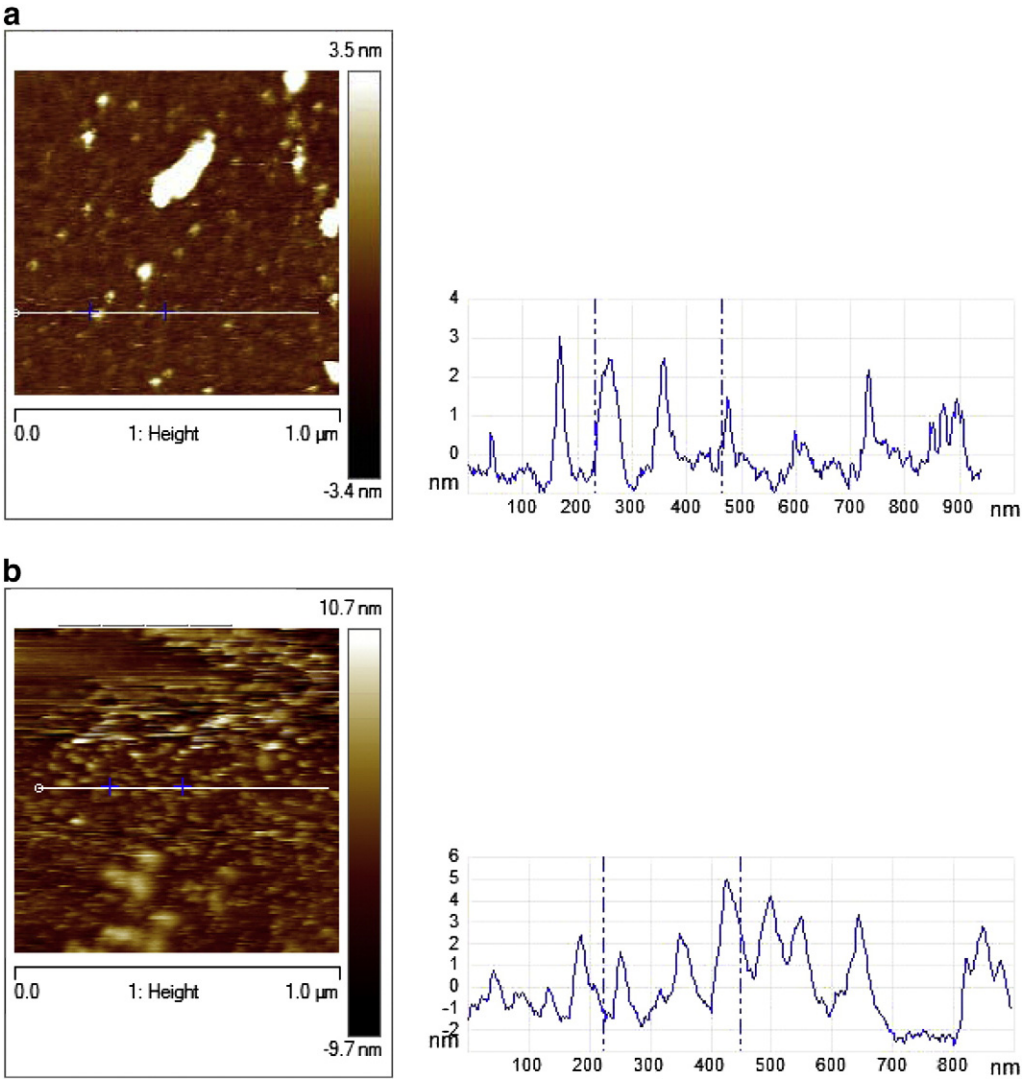

Fig. 4. Images of POPC bilayer after incubation with (a) 0, (b) 2, (c) 4, (d) 8, and (e) 20 μM G_5-COOH PAMAM dendrimers with representative section analysis.

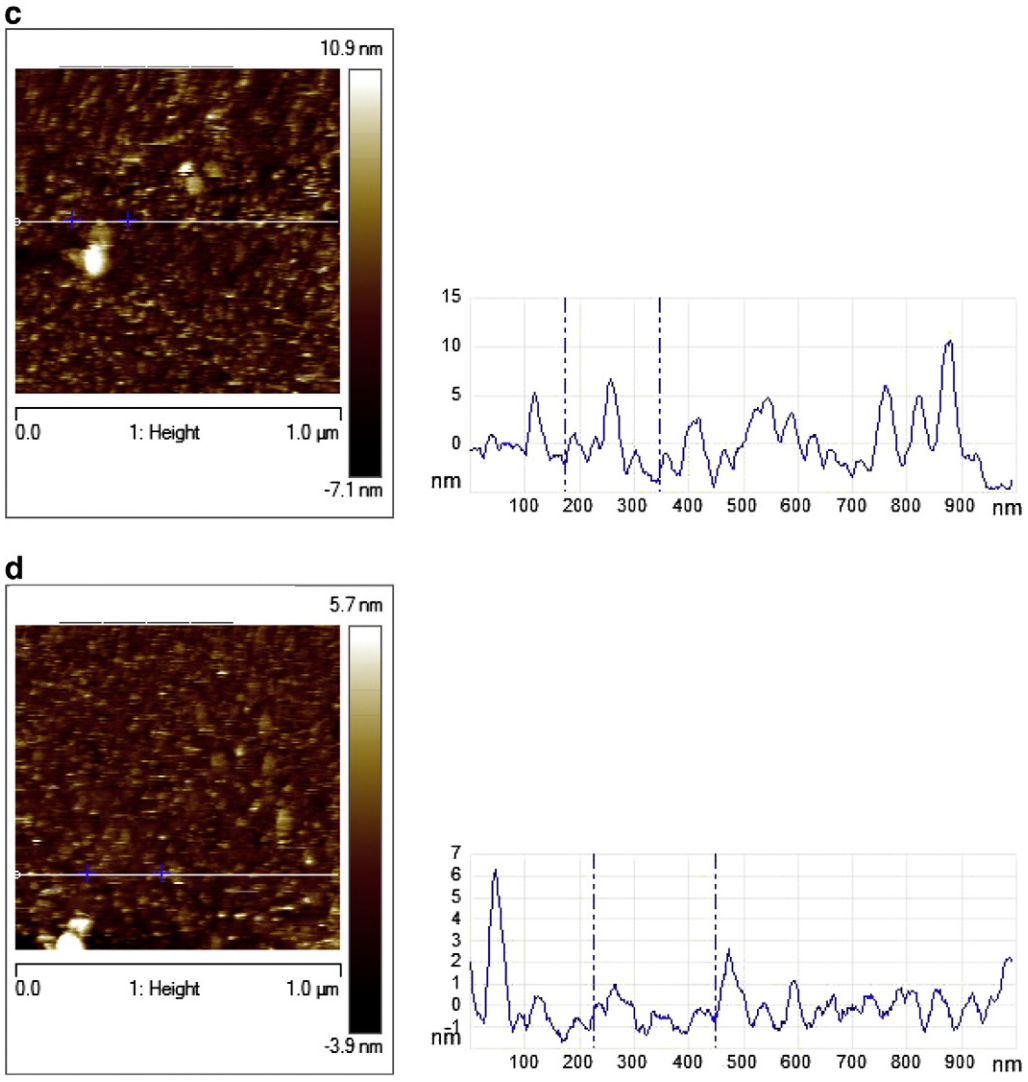

Fig. 4 (*continued*).

As for G_5-COOH, Fig. 4 shows the resulting POPC SPB during exposure to G_5-COOH. Small protrusions (typically less than 3 nm in height; Fig. 4a) formed after exposure to 2 μM G_5-COOH. The development of the protrusions also resulted in surface roughness increasing from 0.23 nm to 1.3 nm. Exposing the bilayer to 4 μM G_5-COOH produced a multitude of bilayer protrusions that ranged in height (4–10 nm), resulting in an increased surface roughness of 2.11 nm (Fig. 4c). Fig. 4d depicts the bilayer during exposure to 8 μM G_5-COOH. The bilayer was left with seemingly an increased number of protrusions that were as tall as 14 nm, but mostly around or below 7 nm high. The surface roughness increased to 2.67 nm. However, as seen in Fig. 4e, the protrusions became smaller (<5 nm tall) during the bilayer's exposure to 20 μM G_5-COOH. The smaller protrusions resulted in a reduction of the surface roughness to nearly 1 nm. This was probably due to the increased frequency with which the protrusions appeared and due to crowding (each protrusion limited the size of its nearest neighbors).

3.3. QCM-D measurements

Zwitterionic POPC was the chosen lipid for evaluating carboxyl-terminated G_2-COOH and G_5-COOH PAMAM dendrimers interacting with a SPB. Upon exposing the silica to POPC liposomes, a SPB was formed in the typical two-step process (Fig. 5) found for liposomes adsorbing onto silica at or above their phase transition temperature in salt-buffer solutions [45–47]. The final Δf and ΔD were approximately −22.4 Hz and $0.16 * 10^{-6}$ (3rd overtone), respectively. This was well within range of final frequency and dissipation shifts found for POPC liposomes [48] and other phosphatidylcholine liposomes adsorbing onto silica [38].

Figs. 5 and 6 depict the profiles of Δf and ΔD during interaction of carboxyl-terminated G_2-COOH and G_5-COOH with a POPC supported bilayer, respectively. During the exposure of POPC SPB to G_2-COOH (Fig. 5), there was no appreciable decrease in Δf, indicating that no mass adsorbed onto the SPB (thus, G_2-COOH did not adsorb to the bilayer). On the other hand, there was a small increase in Δf and ΔD (final ΔD values remained well below 10^{-6}), indicating a slight mass loss and increased softness. Dissipation values, however, remained below 1 which indicated that the Sauerbrey equation remained appropriate for analysis. Thus, the slight Δf increase translated into a small net mass loss (~408 ± 18 ng/cm^2 before exposure; ~384 ± 26 ng/cm^2 after rinse). Assuming a slight mass loss, then this net mass loss translates into about 94% of the original mass remaining intact, clearly showing no G_2-COOH adsorbed. This is consistent with the AFM images that showed small defects had formed in the POPC SPB while exposed to G_2-COOH and explains the leakage data (small defects resulted in leakage, but not catastrophic disruption of the bilayer). Additionally, the findings here that G_2-COOH created non-catastrophic defects in phosphatidylcholine bilayer are similar

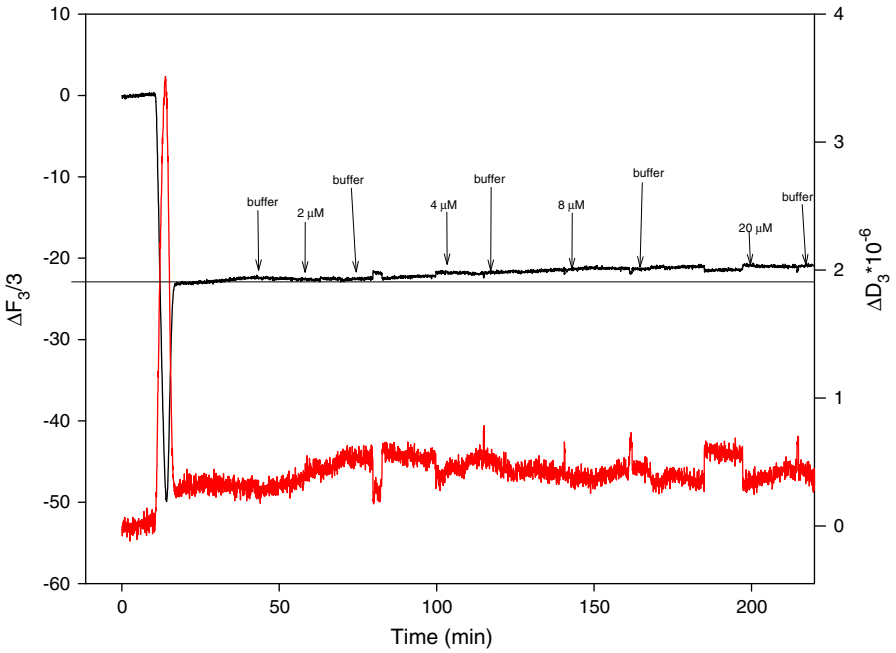

Fig. 5. Typical QCM-D response after 2, 4, 8, and 20 μM G_2-COOH PAMAM dendrimers interacted with a POPC bilayer in 10 mM HEPES, pH 7.4. The arrows indicate buffer and G_2-COOH injections.

to those presented by Mecke et al. (2004) [31] where they found carboxyl-terminated dendrimers to attack the edges of defects but not be catastrophic to the bilayer. It should be noted that their work was done with 1,2-dimyristoylphosphatidylcholine (DMPC) bilayers in unbuffered saline solution with generation 7 dendrimers.

In relationship to other similar works, the net mass loss observed here is small when compared to the net mass loss (~150 ng/cm^2) measured by Parimi et al. (2008) for 100 nM amine-terminated G_2 [21] interacting with DMPC bilayers in a similar HEPES-based buffer (10 mM HEPES, pH 7.4 with or without saline). This was not surprising considering that amine-terminated PAMAM was found to be more disruptive to phospholipid membranes than carboxyl-terminated PAMAM in comparative studies [29,31,32]. Therefore, it is reasonable to expect NH_3^+-terminated G2 to be more potent at lower concentrations than G_2-COOH PAMAM. Overall, leakage and QCMD data in this work indicated that G_2-COOH interacted with a POPC SPB in a rapid, dynamical but weak nature, generating defects. This work also demonstrated that G_2-COOH PAMAM dendrimers did not have to penetrate the bilayer to induce leakage, similar to the results found by Akesson et al. (2012) [49] where they demonstrated that PAMAM G6 dendrimers could induce leakage without penetrating the liposome lumen.

As Fig. 6 depicts, G_5-COOH adsorption clearly resulted in the addition of mass as the POPC bilayer was exposed to 2 to 20 μM G_5-COOH as evident by Δf decreasing to a final value of approximately −29 Hz. From 2 to 4 μM, the added mass remained a rigid film as indicated

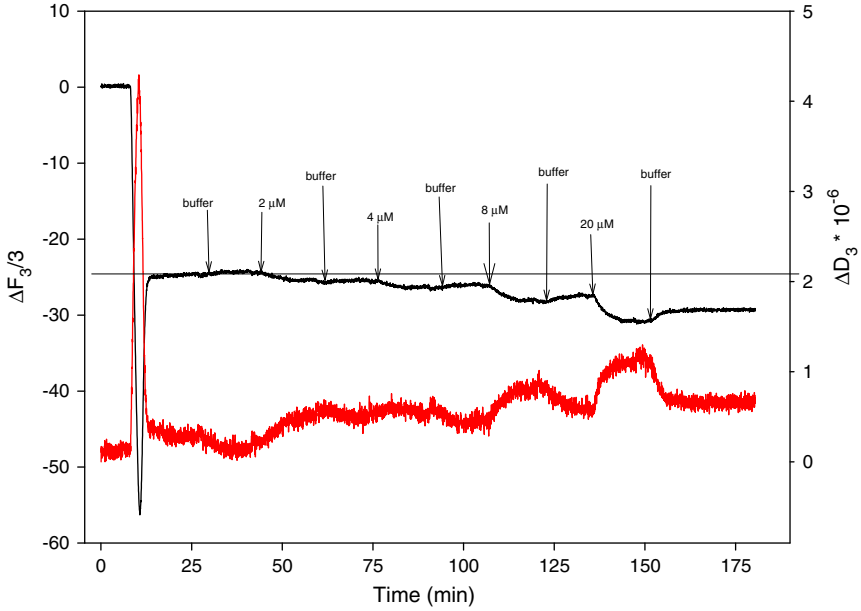

Fig. 6. Typical QCM-D response after the adsorption of 2, 4, 8, and 20 μM G_5-COOH PAMAM dendrimers onto a POPC bilayer in 10 mM HEPES, pH 7.4. G_5-COOH and buffer injections are indicated by arrows above the frequency shift — black line.

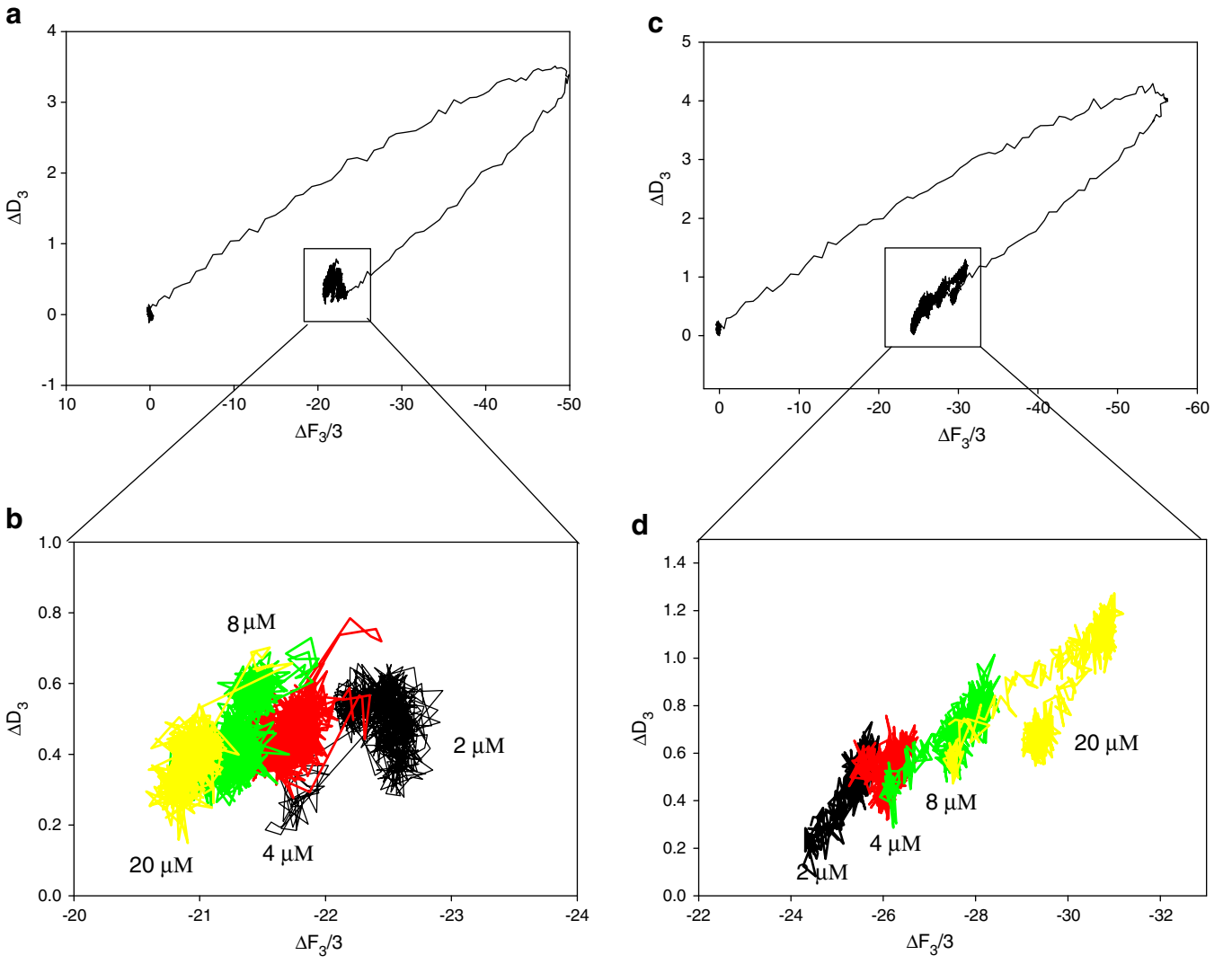

Fig. 7. ΔD vs Δf plots of G_2-COOH and G_5-COOH adsorption onto POPC bilayers: (a,c) adsorption process of POPC liposomes and dendrimers; (b,d) enlargement of adsorption process of G_2-COOH and G_5-COOH, respectively. The colors are used (b,d) to emphasize each dendrimer concentration addition (2 μM — black, 4 μM — red, 8 μM — green, 20 μM — yellow); displayed data were reduced to every 5th point for clarity.

by ΔD value around $0.4 * 10^{-6}$. With each exposure to G_5-COOH above 4 μM, the bilayer became more dissipative. This is in good agreement with the AFM images that show increased local swelling on the bilayer surface after exposure to increased amounts of G_5-COOH. It was also noted that there was a slight increase in Δf after each subsequent buffer rinse, indicating that the frequency shifts were partially due to G_5-COOH in the bulk liquid.

Additional information was gleaned by displaying ΔD versus Δf, which removes time as an explicit parameter of the adsorption process, providing a direct correlation of energy dissipation (ΔD) and adsorbed mass (Δf) [49,50]. Fig. 7a and c depicts the full adsorption process of POPC liposomes and dendrimers. Clearly POPC liposomes exhibited the typical restructuring found for intact liposome adsorption and subsequent rupturing on silica surfaces [51] and agreed well with the behavior previously reported for POPC liposome fusion on silica [52]. Depicted in Fig. 7b and d are the ΔD–Δf plots for G_2-COOH and G_5-COOH adsorption, respectively. In Fig. 7b it was clearly noticed that no mass was added during the interaction of each concentration of G_2-COOH (depicted by an individual color). Second, the slopes of the ΔD–Δf plots for G_2-COOH were not well defined, which suggested that no structural changes occurred and contributions made by G_2-COOH interaction with the bilayer were more to the frequency shift than to the dissipation shift [52]. Finally, the plot shows a clear but marginal shift toward lower ΔD and lower Δf after each subsequent concentration injection. This indicated that each subsequent G_2-COOH injection resulted in slight mass displacement that left the bilayer marginally more rigid. The small mass loss could be small amounts of lipids [53] and/or water.

In Fig. 7d it was noticed that the slopes of the ΔD–Δf plot for G_5-COOH are well-defined and each injection had two linear sections nearly parallel to one another. This indicates several things. First, the sections of ΔD–Δf per injection after rinsing indicate that more energy is associated with dissipation changes and not frequency for each injection of G_5-COOH. Secondly, the near parallel behavior of each injection indicates that each injection interacted similarly with the bilayer. In other words, there was no concentration dependent structural rearrangement of G_5-COOH as it encountered the membrane. Finally, the ΔD–Δf plot clearly shows that each injection and adsorption of G_5-COOH led to a less rigid layer. Analysis of the (G_5-COOH adsorbed) bilayer thickness showed the bilayer changed from 5 nm to ~7 nm (data not shown). This agrees well with AFM section analysis of locally swollen bilayer (Fig. 4). Based on the hydrodynamic radius of G_5-COOH (3 nm) [54], this thickness was less than that expected if G_5-COOH adsorbed on top of the bilayer (~10–11 nm) or that of dendrosomes that may form (~13 nm), as suggested for amine-terminated dendrimers of G2 to G5 [22,28]. It was thus concluded that G_5-COOH

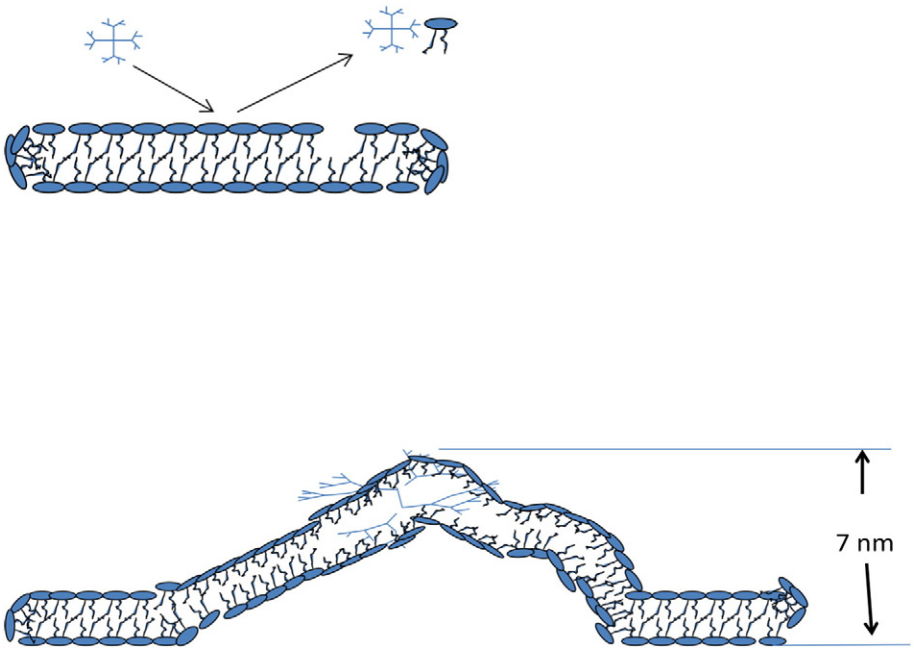

Scheme 1. Representation of G_2-COOH and G_5-COOH interaction with POPC supported phospholipid bilayer. The top panel demonstrates the dynamic nature of the interaction that is believed to occur between G_2-COOH and POPC. The bottom panel illustrates the resultant local bilayer swelling caused by the binding of G_5-COOH to a POPC bilayer.

flattened as it approach the bilayer as seen for G_3 dendrimer by molecular simulations [17].

The difference between the interactions of G_2-COOH and G_5-COOH with POPC bilayer may be explained by molecular model calculations conducted by Kelly et al. (2008) [34]. In their work, models showed that larger dendrimers approaching the liposomal surface extended more than smaller dendrimers. Therefore, it is expected that G_2-COOH would extend less toward a liposomal surface, leaving its core more protected from interactions. However, this does not fully explain the non-adsorption of G_2-COOH to the bilayer, as it would be expected that the negative charge of the G_2-COOH and the zwitterionic characteristic of the bilayer would lead to adsorption [55–57]. A better explanation is that POPC, like DOPC, has an isoelectric value of nearly 4 due to asymmetric binding of hydronium and hydroxide ions [58]. The asymmetric binding of hydronium and hydroxide ions would lead to a varying concentration of hydronium and hydroxide forms of POPC [32], ultimately disturbing effective binding above pH 6.5 [32,59,60]. Our observation that G_2-COOH did not adsorb onto the POPC bilayer is consistent with this theory and agrees with the findings of Zhang et al. (2011). G_5-COOH, on the other hand, would extend more to expose its core and is able to interact more readily with the bilayer because of its exposed hydrophobic core. The exposed core is inserted into the bilayer, inducing the lipids to rearrange near the hydrophobic core. As the core inserts and lipids move to accommodate the dendrimer, water is able to flow across the bilayer. This excess water then pushes again the bilayer, causing the bilayer to curve at the point of dendrimer insertion. Thus, local swelling of the bilayer occurred, entrapping more water. And it is this entrapped extra water that gave the bilayer an increasingly dissipative behavior as evident in QCMD data in Fig. 6. This concept fits with a similar theory [17]. Thus, a model of interaction (Scheme 1) was suggested where G_2-COOH interacts without absorbing to a POPC bilayer but creates small defects, and G_5-COOH penetrated into the bilayer (right), causing the bilayer to swell locally. The implications here are that the best avenue to combine liposomes with either G_2-COOH or G_5-COOH would be to add G_2-COOH to the buffer so as to encapsulate G_2-COOH within the entrapment aqueous contents or embed G_5-COOH within the bilayer membrane.

4. Conclusion

Carboxyl-terminated dendrimers of generations 2 and 5 (G_2-COOH and G_5-COOH, respectively) were explored for their interactions with 1-palmitoyl-2-oleoyl phosphocholine (POPC) bilayers. G_2-COOH PAMAM proved to create increased leakage with increased concentrations in POPC liposomes. Based on QCMD measurements, we believe that carboxyl-terminated G_2-COOH and POPC liposome interaction was dynamic, resulting in local membrane defects that allowed liposomes to leak. This is in contrast to the findings for amine-terminated dendrimers where G_2-NH_2 was found to bind statically within the lipid bilayers and significantly disrupt the bilayer [22,28] On the other hand, G_5-COOH appeared to statistically bind to POPC liposomes, induced increased lipid packing and local swelling. These results indicated a size-dependent interaction of carboxyl-terminated dendrimers with POPC bilayers. The difference in behavior of G_2-COOH versus G_5-COOH dendrimers may involve accessibility of the dendrimer core where G_2-COOH extends less and has lower asphericity (maintains its spherical nature) which resulted in less interaction with the membrane; G_5-COOH, on the other hand, extends more to have greater asphericity so that it binds irreversibly and is flat to the bilayer.

Acknowledgements

The authors are indebted to Nathan Whitman for his technical assistance.

References

[1] Y. Namiki, T. Fuchigami, N. Tada, R. Kawamura, S. Matsunuma, Y. Kitamoto, M. Nakagawa, Nanomedicine for cancer: lipid-based nanostructures for drug delivery and monitoring, Acc. Chem. Res. 44 (2011) 1080–1093.
[2] R.H.H. Neubert, Potentials of new nanocarriers for dermal and transdermal drug delivery, Eur. J. Pharm. Biopharm. 77 (2011) 1–2.
[3] S. Nguyen, S.J. Alund, M. Hiorth, A.-L. Kjøniksen, G. Smistad, Studies on pectin coating of liposomes for drug delivery, Colloids Surf. B: Biointerfaces 88 (2011) 664–673.

[4] J.A. Zasadzinski, B. Wong, N. Forbes, G. Braun, G. Wu, Novel methods of enhanced retention in and rapid, targeted release from liposomes, Curr. Opin. Colloid Interface Sci. 16 (2011) 203–214.
[5] L. Albertazzi, B. Storti, L. Marchetti, F. Beltram, Delivery and subcellular targeting of dendrimer-based fluorescent pH sensors in living cells, J. Am. Chem. Soc. 132 (2010) 18158–18167.
[6] W. Cao, L. Zhu, Synthesis and unimolecular micelles of amphiphilic dendrimer-like star polymer with various functional surface groups, Macromolecules 44 (2011) 1500–1512.
[7] L. Jia, J.-P. Xu, H. Wang, J. Ji, Polyamidoamine dendrimers surface-engineered with biomimetic phosphorylcholine as potential drug delivery carriers, Colloids Surf. B: Biointerfaces 84 (2011) 49–54.
[8] S. Svenson, Dendrimers as versatile platform in drug delivery applications, Eur. J. Pharm. Biopharm. 71 (2009) 445–462.
[9] G.M. El Maghraby, B.W. Barry, A.C. Williams, Liposomes and skin: from drug delivery to model membranes, Eur. J. Pharm. Sci. 34 (2008) 203–222.
[10] M.N. Sarbolouki, M. Sadeghizadeh, M.M. Yaghoobi, A. Karami, T. Lohrasbi, Dendrosomes: a novel family of vehicles for transfection and therapy, J. Chem. Technol. Biotechnol. 75 (2000) 919–922.
[11] M.F. Ottaviani, R. Daddi, M. Brustolon, N.J. Turro, D.A. Tomalia, Structural modifications of DMPC vesicles upon interaction with poly(amidoamine) dendrimers studied by CW-electron paramagnetic resonance and electron spin-echo techniques, Langmuir 15 (1999) 1973–1980.
[12] Z.-Y. Zhang, B.D. Smith, High-generation polycationic dendrimers are unusually effective at disrupting anionic vesicles: membrane bending model, Bioconjug. Chem. 11 (2000) 805–814.
[13] M.F. Ottaviani, P. Matteini, M. Brustolon, N.J. Turro, S. Jockusch, D.A. Tomalia, Characterization of starburst dendrimers and vesicle solutions and their interactions by CW- and pulsed-EPR, TEM, and dynamic light scattering, J. Phys. Chem. B 102 (1998) 6029–6039.
[14] S. Hong, A.U. Bielinska, A. Mecke, B. Keszler, J.L. Beals, X. Shi, L. Balogh, B.G. Orr, J.R. Baker, M.M. BanaszakHoll, Interaction of poly(amidoamine) dendrimers with supported lipid bilayers and cells: hole formation and the relation to transport, Bioconjug. Chem. 15 (2004) 774–782.
[15] A. Mecke, D.-K. Lee, A. Ramamoorthy, B.G. Orr, M.M. Banaszak Holl, Synthetic and natural polycationic polymer nanoparticles interact selectively with fluid-phase domains of DMPC lipid bilayers, Langmuir 21 (2005) 8588–8590.
[16] A. Mecke, I.J. Majoros, A.K. Patri, J.R. Baker, M.M. Banaszak Holl, B.G. Orr, Lipid bilayer disruption by polycationic polymers: the roles of size and chemical functional group, Langmuir 21 (2005) 10348–10354.
[17] C.V. Kelly, P.R. Leroueil, B.G. Orr, M.M. Banaszak Holl, I. Andricioaei, Poly(amidoamine) dendrimers on lipid bilayers II: effects of bilayer phase and dendrimer termination, J. Phys. Chem. B 112 (2008) 9346–9353.
[18] B. Klajnert, J. Janiszewska, Z. Urbanczyk-Lipkowska, M. Bryszewska, R.M. Epand, DSC studies on interactions between low molecular mass peptide dendrimers and model lipid membranes, Int. J. Pharm. 327 (2006) 145–152.
[19] B. Klajnert, R.M. Epand, PAMAM dendrimers and model membranes: differential scanning calorimetry studies, Int. J. Pharm. 305 (2005) 154–166.
[20] K. Gardikis, S. Hatziantoniou, K. Viras, M. Wagner, C. Demetzos, A DSC and Raman spectroscopy study on the effect of PAMAM dendrimer on DPPC model lipid membranes, Int. J. Pharm. 318 (2006) 118–123.
[21] S. Parimi, T.J. Barnes, C.A. Prestidge, PAMAM dendrimer interactions with supported lipid bilayers: a kinetic and mechanistic investigation, Langmuir 24 (2008) 13532–13539.
[22] C.V. Kelly, M.G. Liroff, L.D. Triplett, P.R. Leroueil, D.G. Mullen, J.M. Wallace, S. Meshinchi, J.R. Baker, B.G. Orr, M.M. Banaszak Holl, Stoichiometry and structure of poly(amidoamine) dendrimer–lipid complexes, ACS Nano 3 (2009) 1886–1896.
[23] A.J. Khopade, F. Caruso, P. Tripathi, S. Nagaich, N.K. Jain, Effect of dendrimer on entrapment and release of bioactive from liposomes, Int. J. Pharm. 232 (2002) 157–162.
[24] A. Papagiannaros, K. Dimas, G.T. Papaioannou, C. Demetzos, Doxorubicin–PAMAM dendrimer complex attached to liposomes: cytotoxic studies against human cancer cell lines, Int. J. Pharm. 302 (2005) 29–38.
[25] M.L. Moraes, M.S. Baptista, R. Itri, V. Zucolotto, O.N. Oliveira Jr., Immobilization of liposomes in nanostructured layer-by-layer films containing dendrimers, Mater. Sci. Eng. C 28 (2008) 467–471.
[26] K. Gardikis, S. Hatziantoniou, M. Signorelli, M. Pusceddu, M. Micha-Screttas, A. Schiraldi, C. Demetzos, D. Fessas, Thermodynamic and structural characterization of liposomal-locked in-dendrimers as drug carriers, Colloids Surf. B: Biointerfaces 81 (2010) 11–19.
[27] M.-L. Ainalem, R.A. Campbell, S. Khalid, R.J. Gillams, A.R. Rennie, T. Nylander, On the ability of PAMAM dendrimers and dendrimer/DNA aggregates to penetrate POPC model biomembranes, J. Phys. Chem. B 114 (2010) 7229–7244.
[28] P.R. Leroueil, S.A. Berry, K. Duthie, G. Han, V.M. Rotello, D.Q. McNerny, J.R. Baker, B.G. Orr, M.M. Banaszak Holl, Wide varieties of cationic nanoparticles induce defects in supported lipid bilayers, Nano Lett. 8 (2008) 420–424.
[29] N. Malik, R. Wiwattanapatapee, R. Klopsch, K. Lorenz, H. Frey, J.W. Weener, E.W. Meijer, W. Paulus, R. Duncan, Dendrimers: relationship between structure and biocompatibility in vitro, and preliminary studies on the biodistribution of ^{125}I-labelled polyamidoamine dendrimers in vivo, J. Control. Release 65 (2000) 133–148.
[30] P.R. Leroueil, S. Hong, A. Mecke, J.R. Baker, B.G. Orr, M.M. Banaszak Holl, Nanoparticle interaction with biological membranes: does nanotechnology present a Janus face? Acc. Chem. Res. 40 (2007) 335–342.
[31] A. Mecke, S. Uppuluri, T.M. Sassanella, D.-K. Lee, A. Ramamoorthy, J.R. Baker Jr., B.G. Orr, M.M. Banaszak Holl, Direct observation of lipid bilayer disruption by poly(amidoamine) dendrimers, Chem. Phys. Lipids 132 (2004) 3–14.
[32] D. Shcharbin, A. Drapeza, V. Loban, A. Lisichenok, M. Bryszewska, The breakdown of bilayer lipid membranes by dendrimers, Cell. Mol. Biol. Lett. 11 (2006) 242–248.
[33] C.V. Kelly, P.R. Leroueil, E.K. Nett, J.M. Wereszczynski, J.R. Baker, B.G. Orr, M.M. Banaszak Holl, I. Andricioaei, Poly(amidoamine) dendrimers on lipid bilayers I: free energy and conformation of binding, J. Phys. Chem. B 112 (2008) 9337–9345.
[34] J.A. Laszlo, K.O. Evans, K.E. Vermillion, M. Appell, Feruloyl dioleoylglycerol antioxidant capacity in phospholipid vesicles, J. Agric. Food Chem. 58 (2010) 5842–5850.
[35] K.O. Evans, Room-temperature ionic liquid cations act as short-chain surfactants and disintegrate a phospholipid bilayer, Colloids Surf., A Physicochem. Eng. Asp. 274 (2006) 11–17.
[36] M. Rodahl, F. Höök, A. Krozer, P. Brzezinski, B. Kasemo, Quartz crystal microbalance setup for frequency of Q-factor measurements in gaseous and liquid environments, Rev. Sci. Instrum. 66 (1995) 3924–3930.
[37] F. Höök, B. Kasemo, T. Nylander, C. Fant, K. Sott, H. Elwing, Variations in coupled water, viscoelastic properties, and film thickness of a Mefp-1 protein film during adsorption and cross-linking: a quartz crystal microbalance with dissipation monitoring, ellipsometry, and surface plasmon resonance study, Anal. Chem. 73 (2001) 5796–5804.
[38] C.A. Keller, B. Kasemo, Surface specific kinetics of lipid vesicle adsorption measured with a quartz crystal microbalance, Biophys. J. 75 (1998) 1397–1402.
[39] R. Richter, A. Mukhopadhyay, A. Brisson, Pathways of lipid vesicle deposition on solid surfaces: a combined QCM-D and AFM study, Biophys. J. 85 (2003) 3035–3047.
[40] J.A. Laszlo, K.O. Evans, D.L. Compton, M. Appell, Dihydrolipoyl dioleoylglycerol antioxidant capacity in phospholipid vesicles, Chem. Phys. Lipids 165 (2012) 160–168.
[41] N. Karoonuthaisiri, K. Titiyevskiy, J.L. Thomas, Destabilization of fatty acid-containing liposomes by polyamidoamine dendrimers, Colloids Surf. B: Biointerfaces 27 (2003) 365–375.
[42] A.H. Krall, D.A. Weitz, Internal dynamics and elasticity of fractal colloidal gels, Phys. Rev. Lett. 80 (1998) 778–781.
[43] A. Åkesson, C.V. Lundgaard, N. Ehrlich, T.G. Pomorski, D. Stamou, M. Cárdenas, Induced dye leakage by PAMAM G6 does not imply dendrimer entry into vesicle lumen, Soft Matter 8 (2012) 8972–8980.
[44] L.M. Hays, J.H. Crowe, W. Wolkers, S. Rudenko, Factors affecting leakage of trapped solutes from phospholipid vesicles during thermotropic phase transitions, Cryobiology 42 (2001) 88–102.
[45] H.P. Wacklin, Composition and asymmetry in supported membranes formed by vesicle fusion, Langmuir 27 (2011) 7698–7707.
[46] T. Zhu, F. Xu, B. Yuan, C. Ren, Z. Jiang, Y. Ma, Effect of calcium cation on lipid vesicle deposition on silicon dioxide surface under various thermal conditions, Colloids Surf. B: Biointerfaces 89 (2012) 228–233.
[47] E. Reimhult, B. Kasemo, F. Höök, Rupture pathway of phosphatidylcholine liposomes on silicon dioxide, Int. J. Mol. Sci. 10 (2009) 1683–1696.
[48] I. Pfeiffer, B. Seantier, S. Petronis, D. Sutherland, B. Kasemo, M. Zach, Influence of nanotopography on phospholipid bilayer formation on silicon dioxide, J. Phys. Chem. B 112 (2008) 5175–5181.
[49] X. Zhang, S. Yang, Nonspecific adsorption of charged quantum dots on supported zwitterionic lipid bilayers: real-time monitoring by quartz crystal microbalance with dissipation, Langmuir 27 (2011) 2528–2535.
[50] F. Höök, M. Rodahl, P. Brzezinski, B. Kasemo, Energy dissipation kinetics for protein and antibody–antigen adsorption under shear oscillation on a quartz crystal microbalance, Langmuir 14 (1998) 729–734.
[51] E. Reimhult, F. Höök, B. Kasemo, Intact vesicle adsorption and supported biomembrane formation from vesicles in solution: influence of surface chemistry, vesicle size, temperature, and osmotic pressure, Langmuir 19 (2003) 1681–1691.
[52] M. Sundh, S. Svedhem, D.S. Sutherland, Formation of supported lipid bilayers at surfaces with controlled curvatures: influence of lipid charge, J. Phys. Chem. B 115 (2011) 7838–7848.
[53] K. El Kirat, S. Morandat, Y.F. Dufrêne, Nanoscale analysis of supported lipid bilayers using atomic force microscopy, Biochim. Biophys. Acta, Gen. Subj. 1798 (2010) 750–765.
[54] B. Fritzinger, U. Scheler, Scaling behaviour of PAMAM dendrimers determined by diffusion NMR, Macromol. Chem. Phys. 206 (2005) 1288–1291.
[55] B. Wang, L. Zhang, S.C. Bae, S. Granick, Nanoparticle-induced surface reconstruction of phospholipid membranes, Proc. Natl. Acad. Sci. 105 (2008) 18171–18175.
[56] Y. Yu, S.M. Anthony, L. Zhang, S.C. Bae, S. Granick, Cationic nanoparticles stabilize zwitterionic liposomes better than anionic ones, J. Phys. Chem. C 111 (2007) 8233–8236.
[57] Y. Li, N. Gu, Thermodynamics of charged nanoparticle adsorption on charge-neutral membranes: a simulation study, J. Phys. Chem. B 114 (2010) 2749–2754.
[58] R. Zimmermann, D. Küttner, L. Renner, M. Kaufmann, J. Zitzmann, M. Müller, C. Werner, Charging and structure of zwitterionic supported bilayer lipid membranes studied by streaming current measurements, fluorescence microscopy, and attenuated total reflection Fourier transform infrared spectroscopy, Biointerphases 4 (2009) 1–6.
[59] I. Brzozowska, Z.A. Figaszewski, The influence of pH on phosphatidylcholine monolayer at the air/aqueous solution interface, Colloids Surf. B: Biointerfaces 27 (2003) 303–309.
[60] P.J. Quinn, R.M.C. Dawson, The pH dependence of calcium adsorption onto anionic phospholipid monolayers, Chem. Phys. Lipids 8 (1972) 1–9.